Solar Energy 191 (2019) 1–6

Contents lists available at ScienceDirect

Solar Energy

journal homepage: www.elsevier.com/locate/solener

Photoelectrochemical performance of spray-deposited Fe-doped $ZnS_{0.2}Se_{0.8}$ thin films

Nandkishor M. Patil, Santosh G. Nilange, Abhijit A. Yadav*

Thin Film Physics Laboratory, Department of Physics, Electronics and Photonics, Rajarshi Shahu Mahavidyalaya, Latur (Autonomous) 413512, Maharashtra, India

ARTICLE INFO

Keywords:
Doping
N-type conductivity
PEC cell parameters
Barrier height
Spectral response

ABSTRACT

Binary and ternary II–VI group semiconductor compounds are materials with potential use in various optoelectronic applications, including photoelectrochemical (PEC) solar cells. Thin films of $ZnS_{0.2}Se_{0.8}$ with various Fe-doping concentrations were successfully deposited on fluorine-doped tin oxide-coated glass substrates at a deposition temperature of 275 °C using the chemical spray pyrolysis. PEC cells with Fe:$ZnS_{0.2}Se_{0.8}$ thin film/1 M polysulphide/C (graphite) configurations were designed, and the effect of Fe doping on the PEC performance was studied. The results showed that Fe doping in $ZnS_{0.2}Se_{0.8}$ enhanced the performance of the PEC cells significantly. The optimum concentration was 0.20 mol%. The flat band potential and junction barrier height were maximum at this concentration, with values of −1.18 V and 0.27 eV, respectively. The junction ideality factors of the 0.20 mol% Fe-doped $ZnS_{0.2}Se_{0.8}$ thin film-based PEC cell in the dark and under illumination were found to be 1.21 and 1.17, respectively. The photovoltaic power output characteristics were boosted by Fe doping with a concentration of 0.20 mol%, with the open circuit voltage being 320 mV and the short circuit current being 1.48 mA cm^{-2}. The solar-to-electrical conversion and the fill factor of the 0.20 mol% Fe-doped $ZnS_{0.2}Se_{0.8}$ thin film-based PEC cells were superior, with values of 2.84% and 0.60, respectively. A PEC cell with a 0.20 mol% Fe-doped $ZnS_{0.2}Se_{0.8}$ photosensitive thin film had the highest spectral sensitivity, at a wavelength of 375 nm, with an optical band gap of 3.30 eV.

1. Introduction

Energy is necessary for any living creature. It is a vital element of human life, playing a crucial role in the socio-economic development of the world. Today, the world power utilization is approximately 13 TW, more than 80% of which is generated from non-renewable energy sources such as coal, oil, and natural gas. The worldwide energy demand has been accelerating at an alarming rate, rapidly depleting fossil fuel-based energy stocks and driving a search for clean and safe alternative energy sources. Solar energy is one of the most promising available renewable energy sources, the use of which involves the conversion of light energy directly to electrical energy. It is freely available, abundant, and environment-friendly (carbon-free). The solar energy available is approximately 10,000 times more than the annual energy requirements of the world (Iqbal and Rehman, 2018; Liu and Wang, 2019; Arutyunov and Lisichkin, 2017). Thus it is important to search for and develop solar energy conversion technologies that are efficient, simple, affordable, clean, and eco-friendly in order to meet present and future green energy demands (Karim et al., 2019).

There are two types of semiconductor-based solar cells: solid–solid junction solar cells and solid–liquid junction solar cells. The photoelectrochemical cell (PEC) is a simple type of solar cell in which a solid–liquid junction can be utilized for the energy conversion. PEC devices are affordable and easy to fabricate. PEC cells are promising devices. It might be possible to develop inexpensive photovoltaic panels by enhancing the power conservation efficiency of PEC devices. Thus many researchers have worked on the use of PEC techniques for electricity generation (Baig et al., 2019; Hodes, 1980; Ansari et al., 2019).

The semiconducting material is a key component in a PEC solar cell. It absorbs incident photons and creates electron–hole pairs (van de Krol, 2018). II–VI group semiconducting materials, with broad direct optical band gaps, have excellent optical and electrical properties that are suitable for the fabrication of many optoelectronic devices such as photovoltaic cells and PEC cells (Isshiki and Wang, 2017; Manivannan and Noyel Victoria, 2018). Among the various II–VI group semiconductors, ZnS- and ZnSe-based binary and ternary compounds have been found to be important materials for fabrication of optoelectronic devices (Fard and Dehghani, 2019; Bechiri et al., 2009). ZnS_xSe_{1-x} are important ternary compounds that have received a lot of attention because they offer the possibility of tuning significant parameters such

* Corresponding author.
E-mail address: aay_physics@yahoo.co.in (A.A. Yadav).

https://doi.org/10.1016/j.solener.2019.08.052
Received 7 July 2019; Received in revised form 14 August 2019; Accepted 20 August 2019

as the optical band gap (2.70–3.70 eV), lattice constant, and electrical resistivity simply by changing the composition (varying the value of x between 0.0 and 1.0) (Fard and Dehghani, 2019; Mendil et al., 2018; Sadekar et al., 2011). The optical bandgap of these compounds is greater than that of CdS, and they are less toxic. All these properties make ZnS_xSe_{1-x} suitable for use as buffer layers, which is the undoped region of the solar cell between the doped p-type and n-type layers, in thin film heterojunction solar cells in place of the harmful conventionally used CdS (Venkata Subbaiah et al., 2007; Chen and Dai, 2017).

Venkata Subbaiah et al. (2008) reported a power conversion efficiency of 1.6% for $ZnS_{0.5}Se_{0.5}$ buffer-based thin films synthesized at 300 °C using the close-spaced evaporation method. Previously we grew ZnS_xSe_{1-x} ($0.0 \leq x \leq 1.0$) thin films using the chemical spray pyrolysis technique (Patil et al., 2019). We found that a PEC cell with a $ZnS_{0.2}Se_{0.8}$ photoelectrode had the maximum photon-to-electrical conversion efficiency (1.27%) and the least resistivity (Patil et al., 2019). However, the photon-to-electrical conversion efficiency is considerably lower. The higher electrical resistivity of the photoelectrode is responsible for the poor photon conversion efficiency of the PEC cell. The electrical resistivity can be reduced considerably simply by adding a small amount of a suitable impurity or dopant. Both the open circuit voltage and the short circuit current rise significantly due to doping. Hence, the efficiency of PEC cells can be easily and effectively improved with a suitable dopant (Yadav et al., 2011; Yadav and Masumdar, 2011; Bhuse et al., 2007; Saikia et al., 2016).

Siddiqui and colleagues (Siddiqui et al., 2017) observed that $CdS_{0.8}Se_{0.2}$ thin films doped with a Cu impurity can be used to fabricate heterojunction solar cells and that the efficiency of such heterojunction solar cell is boosted by the Cu-doped thin films. Bhuse and co-workers (Bhuse et al., 2007) observed that indium as a dopant had a strong influence on the PEC properties of $Cd_{0.6}Hg_{0.4}Se$ thin films prepared using the chemical bath deposition (CBD) method. They reported that various PEC parameters of the $Cd_{0.6}Hg_{0.4}Se$ thin films, including the open circuit voltage, short circuit current, fill factor, and photon-to-electrical conversion efficiency were boosted by the indium dopant. Lohar et al. (2015) observed that the overall performance of a PEC cell with ZnSe nano-needles effectively improves when the ZnSe is doped with 1% Fe^{2+}. Trivalent Fe is cheap material and can be used as a dopant to improve the performance of a PEC solar cell.

Various techniques, including screen printing (Kumar and Sharma, 1998), brush plating (Dhanemozhi et al., 2017), thermal evaporation (Ashraf et al., 2009), CBD (Liu et al., 2013), close-spaced evaporation (Venkata Subbaiah et al., 2007), aerosol-assisted chemical vapour deposition (Alghamdi, 2017), dc magnetron sputtering (Ganguly et al., 2001), molecular beam epitaxy (Da-ke et al., 2003), and spray pyrolysis (Ramakrishna Reddy et al., 2003) have been used successfully to grow ZnS_xSe_{1-x} thin films. Foremost among the techniques mentioned in the foregoing for the preparation of high-quality and uniform semiconducting thin films is chemical spray pyrolysis. Spray pyrolysis is one of the easiest adaptable methods for the large-area coating, which is essential for mass production in photovoltaic applications (Franckevičius et al., 2019). The advantages of the technique include its simplicity and affordability. Chemical spray pyrolysis does not require a vacuum system or high-quality substrates or chemicals which are beneficial if the technique is to be scaled up for industrial applications. Also, it is possible to deposit undoped and doped thin films of large area using this technique (Patil et al., 2019, 2018; Perednis et al., 2005; Benramdane et al., 1997; Kamruzzaman et al., 2012).

In the light of our previous work and the findings reported in the literature, we focused on depositing high-quality $ZnS_{0.2}Se_{0.8}$ thin films with different concentrations of ferric chloride hexahydrate dopant (i.e., 0.05, 0.10, 0.20, 0.25, 0.30, 0.50, and 1.00 mol%) onto electrically conductive fluorine-doped tin oxide (FTO)-coated glass substrates at a deposition temperature of 275 °C using the chemical spray pyrolysis technique. We also examined the influence of Fe doping on the performance of PEC cells with a Fe:$ZnS_{0.2}Se_{0.8}$ thin film/1 M polysulphide/C (graphite) configuration.

2. Experimental details

2.1. Chemicals used

AR-grade zinc chloride ($ZnCl_2$), thiourea ($(NH_2)_2CS$), selenourea ($(NH_2)_2CSe$), and dopant ferric chloride hexahydrate ($FeCl_3{\cdot}6H_2O$) were used as sources of Zn, S, Se, and Fe ions, respectively.

2.2. Substrates used

Electrically conductive (sheet resistance 8–10 $\Omega\,cm^{-2}$) FTO-coated glass substrates were used.

2.3. Formation of undoped and Fe-doped $ZnS_{0.2}Se_{0.8}$ electrodes

Ferric chloride hexahydrate was used as a Fe^{3+} dopant. Equimolar (0.05 M) aqueous solutions of zinc chloride ($ZnCl_2$, 10 cm^3), thiourea ($(NH_2)_2CS$, 2 cm^3), and selenourea ($(NH_2)_2CSe$, 8 cm^3) and ferric chloride hexahydrate ($FeCl_3{\cdot}6H_2O$) of various concentrations (0.05, 0.10, 0.20, 0.25, 0.30, 0.50, and 1.00 mol%, as a dopant) were used to prepare Fe-doped $ZnS_{0.2}Se_{0.8}$ thin films. When this solution is sprayed onto FTO-coated glass substrates through a glass nozzle at a constant deposition temperature of 275 °C, we get undoped and Fe-doped $ZnS_{0.2}Se_{0.8}$ thin films. The preparative parameters were maintained constant at their optimal values (solution concentration, 0.05 M; spray rate, 3 cm^3 $minute^{-1}$; deposition time, 14–16 min; carrier gas, air at pressure of 176,520 N m^{-2}; distance between substrate and nozzle, 30 cm) for deposition of high-quality undoped and Fe doped $ZnS_{0.2}Se_{0.8}$ thin films. A simple Scotch tape test was used to check the adhesion of the films (Patil et al., 2018, 2019). The PEC properties of the undoped and Fe-doped $ZnS_{0.2}Se_{0.8}$ thin films were examined by constructing PEC cells.

2.4. Construction of undoped and Fe-doped $ZnS_{0.2}Se_{0.8}$ thin film-based PEC solar cells

The experimental setup used for constructing the undoped and Fe-doped $ZnS_{0.2}Se_{0.8}$ thin film-based PEC solar cells has been described by us previously (Patil et al., 2019). A 1 M polysulphide solution was used as a redox electrolyte. PEC cells were fabricated with a standard three-electrode configuration, with Fe-doped $ZnS_{0.2}Se_{0.8}$ thin films acting as the working electrodes and a graphite rod as the counter electrode. A saturated calomel electrode (SCE) was used as a reference electrode. Using the capacitance data, Mott-Schottky (M-S) plots of all the thin films deposited were recorded using an LCR meter (Aplab Model 4912) at a fixed built-in signal frequency of 1 kHz, and these plots were used to determine the flat band potential (V_{fb}) and the donor concentration (N_D) of these films. The photovoltaic power output, i.e., photocurrent density against photo voltage characteristics and current–voltage (I–V) characteristics, were studied in the dark as well as in the presence of light after waiting for sufficient time to equilibrate the system. The junction ideality factors n_d and n_L (in the dark and in the presence of light) were computed from the curve of log I against V. The PEC cells with various Fe-doped $ZnS_{0.2}Se_{0.8}$ thin film photoelectrodes were illuminated with a constant input intensity of 10 mW cm^{-2}. The power output characteristics of the PEC cells were recorded. The fill factor (FF) and photon conversion efficiency (η, as a percentage) of the PEC cell were calculated from the photovoltaic power output characteristics. The barrier height (Φ_b, in electron volts) was determined from the changes in the reverse saturation current at different temperatures. The spectral response characteristics were also recorded.

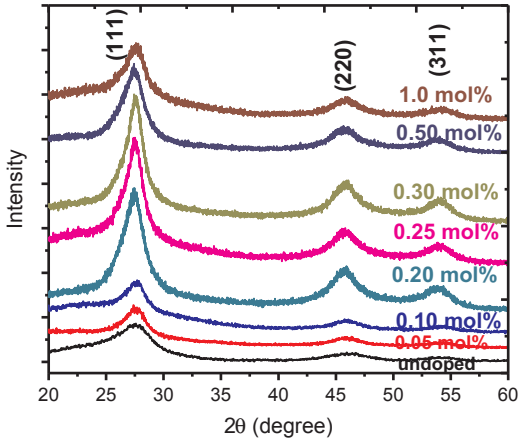

Fig. 1. XRD patterns of spray deposited Fe-doped $ZnS_{0.2}Se_{0.8}$ thin films within 2θ angle 20-60°.

3. Results and discussion

Fig. 1 shows the X-ray diffraction patterns of undoped and Fe doped $ZnS_{0.2}Se_{0.8}$ thin films within 2θ angle 20-60°. From an XRD study, we found that the undoped and Fe doped $ZnS_{0.2}Se_{0.8}$ thin films were polycrystalline and that they had a cubic zinc blende crystal structure. We also observed a preferential orientation along the (1 1 1) plane with a minor shift towards higher 2θ values and a significant change in intensity with increasing Fe-doping in the $ZnS_{0.2}Se_{0.8}$ thin films up to 0.20 mol%. When the Fe doping concentration is increased above 0.20 mol%, there is a slight fall in the intensity of the XRD peaks. The fall in (1 1 1) peak intensity after 0.20 mol% Fe doping might be due the change in electron density or might be due to point defects created due to doping. We found the crystallite size to be in the range 27–35 nm (Table 1). The size was maximum (35 nm) for 0.20 mol% Fe-doped $ZnS_{0.2}Se_{0.8}$. Through an energy-dispersive X-ray spectroscopy study we confirmed that the $ZnS_{0.2}Se_{0.8}$ lattice was doped with Fe ions. Our optical study of all the prepared samples showed that the direct allowed band gap varied according to the Fe-doping concentration and that the 0.20 mol% Fe-doped $ZnS_{0.2}Se_{0.8}$ thin film had a wider band gap (3.25 eV). The electrical resistivity measurements conducted on the Fe-doped $ZnS_{0.2}Se_{0.8}$ thin films showed that the films were semiconducting in nature and that the film doped with 0.20 mol% Fe had the lowest resistivity (0.617×10^5 Ω cm). A thermoelectrical power (TEP) measurement study showed that the type of conductivity of the undoped and Fe doped $ZnS_{0.2}Se_{0.8}$ thin films was the n-type.

3.1. Type of conductivity (n or p)

We checked the type of conductivity (n or p) of the spray deposited undoped and Fe-doped $ZnS_{0.2}Se_{0.8}$ thin films by fabricating PEC cells with the configuration;

Fe:$ZnS_{0.2}Se_{0.8}$thin film/1M polysulphide/C(graphite)

Even in the dark, because of the difference between the two half-cell potentials of the photoelectrode and the graphite counter electrode of the Fe-doped $ZnS_{0.2}Se_{0.8}$ thin films, the PEC cells produced a small voltage and current. It was found that when light struck this semiconductor–electrolyte junction, the magnitude of the open circuit voltage (dark voltage) was enhanced, with the negative polarity towards the Fe-doped $ZnS_{0.2}Se_{0.8}$ thin films. This shows that all the spray deposited thin films were n-type semiconductors (Bhuse, 2007; Patil et al., 2019). These results are consistent with the TEP measurements.

3.2. Capacitance–voltage (C–V) characteristics

The semiconductor–electrolyte interface of a PEC plays a key role in converting solar energy into electrical energy. We gained important information relating to the semiconductor–electrolyte interface, i.e. the solid–liquid junction, from a review by Pandey et al. (1996). The fundamental concepts underlying the charge transfer at an active semiconductor–electrolyte junction are described well in the literature (Ginley and Butler, 1981; Chandra et al., 1986). Fig. 2 shows the C–V characteristics (M-S plots) of the undoped and Fe-doped $ZnS_{0.2}Se_{0.8}$/1 M polysulphide/C (graphite) PEC cells in the dark. From the C–V plots we can determine the donor concentration (N_D), flat band potential (V_{fb}), and type (n or p) of conductivity of the Fe-doped $ZnS_{0.2}Se_{0.8}$ thin films. We carried out Schottky capacitance measurements at a constant frequency of 1 kHz using an LCR meter (Aplab Model 4912) and varying the applied dc bias potential (−0.6 to 0.6 V). The nature of the plots indicates that the undoped and Fe-doped $ZnS_{0.2}Se_{0.8}$ thin films are of the n-type (Murali et al., 2010). The flat band potential (V_{fb}) determines the relative position of the Fermi levels in the photoelectrode and gives the amount of band bending at the Schottky interface (Deshmukh and Shahane, 1997; Hankare et al., 2008). It was measured with respect to a reference electrode and determined at $C_s^{-2} = 0$ on the voltage axis using the following relation, which is known as the M-S relation (Patil et al., 2019):

$$\frac{1}{C_s^2} = \left(\frac{2}{\varepsilon_0 \varepsilon_s q N_D}\right)\left[V - V_{fb} - \left(\frac{kT}{q}\right)\right] \quad (1)$$

In this relation, C_s indicates the space charge capacitance of the thin films, ε_0 is the permittivity of free space, ε_s is the static permittivity of the semiconductor (Fe-doped $ZnS_{0.2}Se_{0.8}$), N_D is the donor concentration (or density), q is the charge of the electron (1.602×10^{-19}C), V represents the applied (i.e., electrode) potential, and T is the absolute temperate (in Kelvin). The estimated V_{fb} values are given in Table 1. The variation of the flat band potential with Fe-doping concentration is presented in Fig. 3. The flat band potential was found to increase from −1.09 V to −1.18 V as the Fe-doping concentration increased from 0 mol% (undoped) to 0.20 mol% and then drop to −1.02 V as the Fe-

Table 1
Estimated important photoelectrochemical parameters of spray deposited Fe-doped $ZnS_{0.2}Se_{0.8}$ thin films.

Doping concentration (mol %)	I_{SC} (μA/cm^2)	V_{OC} (mV)	n_d	n_L	η (%)	FF	Φ_b (eV)	R_S (Ω)	R_{Sh} (kΩ)	N_D (X 10^{19}cm^{-3})	Eg (eV)	D (nm)
0.00	816	268	1.37	1.32	1.27	0.58	0.54	57	3.430	2.87	2.92	28
0.05	952	278	1.28	1.26	1.56	0.59	0.43	45	3.333	3.35	3.10	30
0.10	1211	294	1.23	1.20	2.10	0.59	0.38	33	3.714	6.87	3.10	32
0.20	1477	320	1.21	1.17	2.84	0.60	0.27	31	2.333	7.52	3.30	35
0.25	1309	306	1.22	1.19	2.36	0.59	0.33	29	2.476	7.11	3.20	33
0.30	1099	284	1.25	1.22	1.81	0.58	0.37	32	3.857	6.17	3.10	31
0.50	755	256	1.42	1.39	1.06	0.55	0.61	53	2.625	2.49	2.92	29
1.00	714	245	1.46	1.41	0.94	0.54	0.62	73	3.857	2.01	2.76	27

I_{SC}; short circuit current, V_{OC}; open circuit voltage, n_d; junction ideality factor in dark, n_L; junction ideality factor under illumination, η; efficiency, FF; fill factor, Φ_b; barrier height, R_S; series resistance, R_{Sh}; shunt resistance, N_D; donor concentration, Eg; band gap energy, D; Crystallite size.

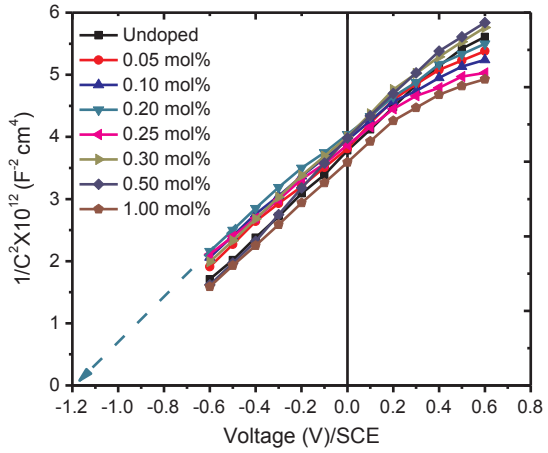

Fig. 2. C–V characteristics of spray deposited undoped and Fe-doped $ZnS_{0.2}Se_{0.8}$ thin films/1 M (Na_2S + S + NaOH)/ C PEC cells with in dark.

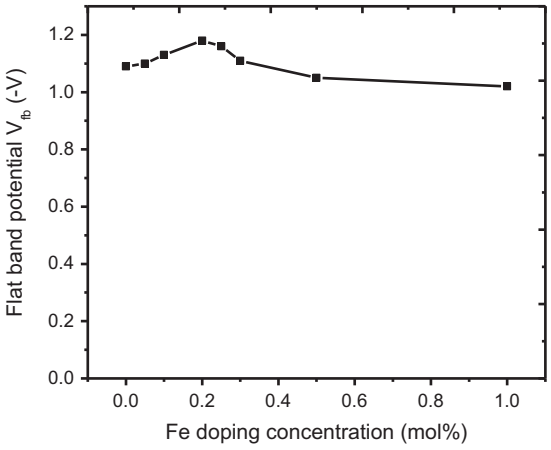

Fig. 3. Variation of flat band potential with Fe doping concentration for spray deposited Fe-doped $ZnS_{0.2}Se_{0.8}$ thin films.

doping increased further, from 0.20 mol% to 1.00 mol%. Clearly, the flat band potential is enhanced by the addition of a Fe impurity and is highest for Fe concentration of 0.20 mol%. The Fe dopant creates a new donor impurity level in the forbidden energy gap of the $ZnS_{0.2}Se_{0.8}$. This donor impurity level shifts the Fermi level up. Hence the band bending increases. This is responsible for the upsurge in the flat band potential. However, with Fe concentrations greater than 0.20 mol%, we observe shrinkage in the flat band potential because of a pinning of the Fermi level (Hankare et al., 2009; Bhuse et al., 2007). The donor densities (N_D) obtained using the M-S relation are of the order of $10^{19}cm^{-3}$ (Table 1), with a maximum value of $7.52 \times 10^{19}cm^{-3}$ at Fe-doping level of 0.20 mol%.

3.3. Current–voltage (I–V) characteristics in the dark and under illumination

Fig. 4 shows the I–V characteristics of the PEC cells with Fe doped $ZnS_{0.2}Se_{0.8}$ thin films in the dark and under illumination (white light). Studying the I–V characteristics is very helpful in understanding the charge transfer process at the electrode–electrolyte junction. The Butler-Volmer relation defines the nature of the charge transport mechanism at the junction (Yadav, 2016). When light falls on the junction, there is a shift in the I–V curve to Quadrant IV, signifying that undoped and Fe-doped $ZnS_{0.2}Se_{0.8}$ thin film-based photoelectrodes can work as electricity generators. The slope of the linear regions of the plots of log I against V (not shown here) provide the junction ideality factors n_d and

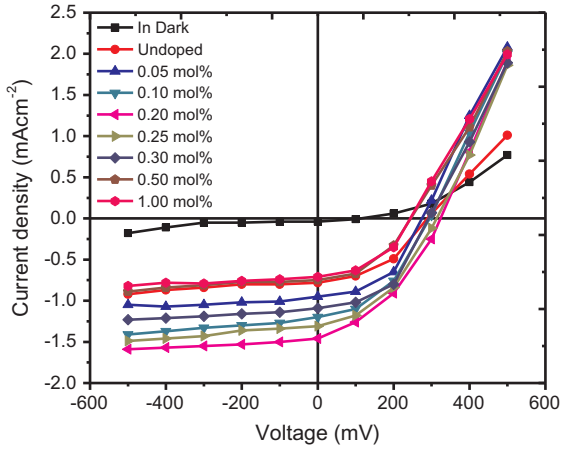

Fig. 4. I–V characteristics of spray deposited undoped and Fe-doped $ZnS_{0.2}Se_{0.8}$/1M (Na_2S + S + NaOH)/C PEC cells in dark and under illumination.

n_L (in the dark and under illumination). These factors were estimated from the well known ideal diode equation (Yadav and Masumdar, 2011). The values obtained are listed in Table 1. The values of n_d and n_L were least (1.21 and 1.17) for the PEC cell with a 0.20 mol% Fe-doped $ZnS_{0.2}Se_{0.8}$ thin film, suggesting that the trap density at the interface was the lowest (Hankare et al., 2009). We observed that these values are close to 1, which suggests that a good quality junction was formed.

3.4. Barrier height (built-in potential) measurements

We estimated the junction barrier height (Φ_b) by measuring the reverse saturation current (I_0) flowing through the Fe:$ZnS_{0.2}Se_{0.8}$ thin film/1 M polysulphide/C junction as a function of the temperature (from 363 K to 303 K). We determined the magnitude of the junction barrier height from the slope of the linear region of the plots of log I_0/T^2 against 1000/T for the Fe:$ZnS_{0.2}Se_{0.8}$ electrodes (Fig. 5). The values obtained are shown in Table 1. From the graph, we saw that the plots were not linear in the high-temperature regions. This nonlinear nature of the plots can be attributed to the Pool-Frankel type of conduction. Hankare and colleagues have observed a similar type of conduction mechanism (Hankare et al., 2009). The junction barrier height (Table 1) decays from 0.54 eV to 0.27 eV as the Fe-doping concentration increases from 0 to 0.20 mol%, and it is lowest (0.27 eV) at 0.20 mol%. It increases to 0.62 eV when the Fe-concentration is increased to 1.00 mol %.

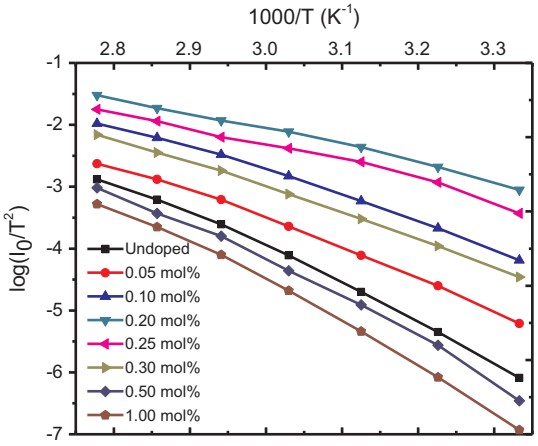

Fig. 5. Plots of log (I_0/T^2) versus 1000/T for spray deposited undoped and Fe doped $ZnS_{0.2}Se_{0.8}$ thin films with various Fe doping concentrations.

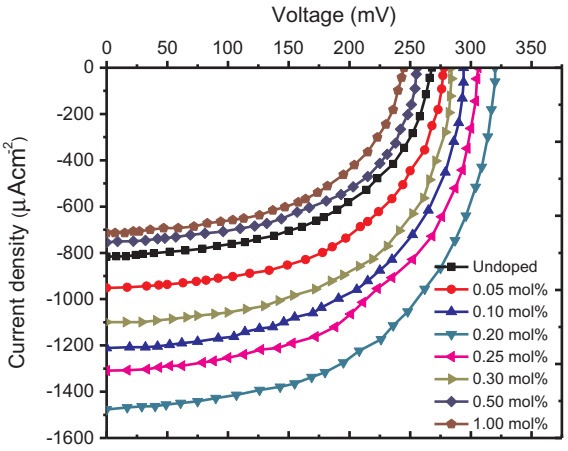

Fig. 6. Power output characteristics for undoped and Fe-doped $ZnS_{0.2}Se_{0.8}$ /1M (Na_2S + S + NaOH)/C PEC cells with various Fe doping concentrations.

3.5. Photovoltaic power output characteristics

The power output characteristics (graph of photocurrent density (in μA cm^{-2}) and photovoltage (in mV)) of the PEC cells with Fe-doped $ZnS_{0.2}Se_{0.8}$ thin films under illumination of constant intensity 10 mW cm^{-2} are shown in Fig. 6.

Fig. 7 shows the variation of the short circuit current (I_{SC}) and the open circuit voltage (V_{OC}) with Fe-doping concentration for the undoped and Fe-doped $ZnS_{0.2}Se_{0.8}$ thin films. As the Fe-doping concentration increases from 0 to 0.20 mol%, both V_{OC} and I_{SC} increase significantly. V_{OC} increases from 268 mV to 320 mV. Similarly, I_{SC} increases from 816 μA cm^{-2} to 1477 μA cm^{-2}. This improves the relevant parameters, such as the photon conversion efficiency and the fill factor (Hankare et al., 2009). As the Fe-doping concentration increases above 0.20 mol%, both V_{OC} and I_{SC} decrease. Both an enhanced V_{fb} and the grain structure of the material are responsible for increasing V_{OC}. On the other hand, I_{SC} improves because of decay in the resistivity of the thin film photoelectrodes (Bhuse et al., 2007; Hankare et al., 2009; Deshmukh et al., 1997).

We computed the PEC performance parameters, namely the fill factor (FF) and the photon-to-electrical conversion efficiency (η, as a percentage), from the power output characteristics using familiar relations given elsewhere (Yadav and Masumdar, 2010). The values we obtained are noted in Table 1. Both the fill factor and the efficiency of the $ZnS_{0.2}Se_{0.8}$ thin films were enhanced when the Fe dopant was introduced. The fill factor increased from 0.58 to 0.60 as the Fe-doping concentration of the $ZnS_{0.2}Se_{0.8}$ thin films increased from 0 to 0.20 mol %. It decreased when the Fe-doping concentration increased above 0.20 mol%. Similarly, the photon-to-electrical conversion efficiency of the fabricated cells was boosted from 1.27% to 2.84% when the Fe-doping concentration increased from 0 to 0.20 mol%. Because of the increase in the magnitude of I_{SC} and V_{OC}, the efficiency and FF were considerably improved (Bhuse et al., 2007). As the doping concentration increases, there is an increase in the number of interfacing sites, which results in enhancement of the number of charge carriers. As a result, we see an improvement in the photon conversion efficiency of the cells (Siddiqui et al., 2017).

We computed the series resistance (R_S) from the slope of the power output characteristics at I = 0 using the following relation:

$$\left(\frac{dI}{dV}\right)_{I=0} \cong \left(\frac{1}{R_s}\right) \tag{2}$$

Similarly, the magnitude of the shunt resistance (R_{Sh}) was calculated from the slope of the power output characteristics at V = 0 using following relation:

$$\left(\frac{dI}{dV}\right)_{V=0} \cong \left(\frac{1}{R_{sh}}\right) \tag{3}$$

The calculated R_S and R_{Sh} of the Fe:$ZnS_{0.2}Se_{0.8}$ thin film/1 M polysulphide/C PEC cells are listed in Table 1. It may be seen from this table that a PEC cell with a 0.20 mol% Fe-doped $ZnS_{0.2}Se_{0.8}$ thin film has the lowest series and shunt resistance values (31 Ω and 2.333 kΩ).

3.6. Spectral response

A spectral response study of the Fe-doped $ZnS_{0.2}Se_{0.8}$ thin films was carried out by measuring I_{SC} as a function of the wavelength of light in the range 300–600 nm. Fig. 8 shows the spectral response curves of the Fe-doped $ZnS_{0.2}Se_{0.8}$/1 M polysulphide/C PECs with various Fe-doping concentrations. From these curves, it is clearly seen that I_{SC} reaches a maximum value at a specific wavelength depending on the Fe-concentration. A PEC cell with a 0.20 mol% Fe-doped $ZnS_{0.2}Se_{0.8}$ photosensitive thin film had the highest spectral sensitivity, at a wavelength of 375 nm, with the optical band gap (Eg) being 3.30 eV. This optical band gap value was approximately the same (i.e., 3.25 eV) as that obtained from the optical absorption studies conducted on these films. The optical band gap values obtained for various Fe concentrations are provided in Table 1. The I_{SC} values decayed as the wavelength grew shorter. This may be because of absorption of light in the electrolyte and large surface recombination of photo-generated minority charge carriers. The non-optimal thickness and transitions between defect

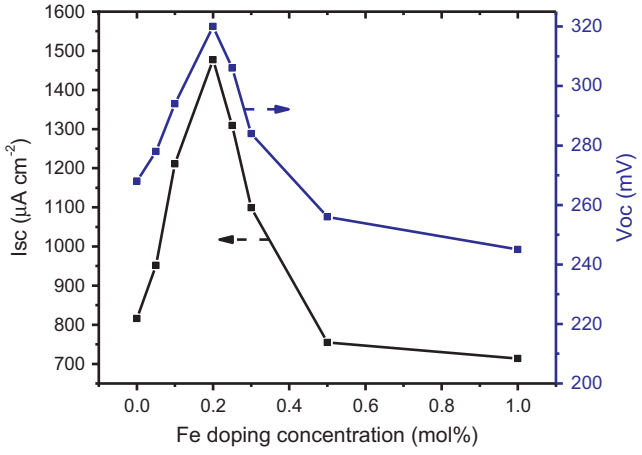

Fig. 7. Variation I_{sc} and V_{oc} with Fe doping concentration for spray deposited undoped and Fe doped $ZnS_{0.2}Se_{0.8}$ thin films.

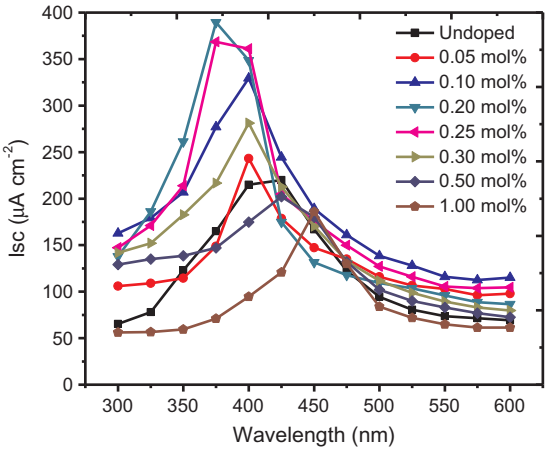

Fig. 8. Spectral response curves for undoped and Fe doped $ZnS_{0.2}Se_{0.8}$/1M (Na_2S + S + NaOH)/C PEC cells with various Fe doping concentrations.

levels cause I_{SC} to decrease with longer wavelengths (Hankare et al., 2009).

4. Conclusions

$ZnS_{0.2}Se_{0.8}$ thin films with various Fe-doping concentrations were successfully deposited on the surface of FTO-coated glass substrates at a temperature of 275 °C using the very simple and inexpensive chemical spray pyrolysis technique. In this study, we examined the effect of Fe-doping on the photoelectrochemical performance of the $ZnS_{0.2}Se_{0.8}$ thin films. All the Fe-doped $ZnS_{0.2}Se_{0.8}$ thin film electrodes were n-type semiconductors. The flat band potential, as determined using the Mott-Schottky relation, changes in accordance with the Fe-doping concentration and reaches the maximum value (−1.18 V) at a concentration of 0.20 mol%. The rectifying nature of the $ZnS_{0.2}Se_{0.8}$/polysulphide interfaces was confirmed from the I–V characteristics. The values of n_d and n_L were lowest (1.21 and 1.17) for the PEC cell formed with a 0.20 mol% Fe-doped $ZnS_{0.2}Se_{0.8}$ thin film, suggesting that the trap density is lowest at the Fe-doped $ZnS_{0.2}Se_{0.8}$/polysulphide interface with this film. The magnitude of the junction barrier height varies from 0.27 eV to 0.62 eV and is lowest (0.27 eV) with Fe-concentration of 0.20 mol%. The photon-to-electrical conversion efficiency and the fill factor were enhanced significantly with increasing Fe-doping concentration. A PEC with a 0.20 mol% Fe-doped $ZnS_{0.2}Se_{0.8}$ thin film has the lowest series and shunt resistance values (31 Ω and 2.333 kΩ, respectively). The spectral response study showed that the spectral sensitivity was high for all the Fe-doped $ZnS_{0.2}Se_{0.8}$ thin films. Our study shows that 0.20 mol% Fe-doped $ZnS_{0.2}Se_{0.8}$ thin films are most suitable for use in PEC cells as electrodes to convert solar energy to electrical energy.

References

Alghamdi, Yousef, 2017. Composition and band gap controlled AACVD of ZnSe and ZnS_xSe_{1-x} thin films using novel single source precursors. Mater. Sci. Appl. 8, 726–737.

Ansari, Mohd Zubair, Singh, Simrjit, Khare, Neeraj, 2019. Visible light active CZTS sensitized CdS/TiO_2 tandem photoanode for highly efficient photoelectrochemical hydrogen generation. Sol. Ener. 181, 37–42.

Arutyunov, Vladimir S., Lisichkin, Georgiy V., 2017. Energy resources of the 21st century: problems and forecasts. Can renewable energy sources replace fossil fuels? Russ. Chem. Rev. 86, 777–804.

Ashraf, M., Akhtar, S.M.J., Mehmood, M., Qayyum, A., 2009. Optical and structural properties of ZnS_xSe_{1-x} thin films deposited by thermal evaporation. Eur. Phys. J. Appl. Phys. 48, 10501–10504.

Baig, Faisal, Khattak, Yousaf Hameed, Jemai, Safa, Soucase, Bernabé Marí, Beg, Saira, 2019. Hydrothermal syntheses of Vanadium doped α-Fe_2O_3 cubic particles with enhanced photoelectrochemical activity. Sol. Ener. 182, 332–339.

Bechiri, A., Benmakhlouf, F., Bouarissab, N., 2009. Calculation of electronic and optical properties of Zn-based II-VI semiconductors. Phy. Procedia 2, 803–812.

Benramdane, N., Murad, W.A., Misho, R.H., Ziane, M., Kebbab, Z., 1997. A chemical method for the preparation of thin films of CdO and ZnO. Mater. Chem. Phy. 48, 119–123.

Bhuse, V.M., 2007. Photo-electrochemical properties of $Cd_{1-x}Hg_xSe$ thin films. Mater. Chem. Phy. 106, 250–255.

Bhuse, V.M., Hankare, P.P., Sonandkar, S., 2007. Structural, optical, electrical and photoelectrochemical studies on indium doped $Cd_{0.6}Hg_{0.4}Se$ thin films. Mater. Chem. Phys. 101, 303–309.

Chandra, S., Singh, S.L., Khare, Neeraj, 1986. A theoretical model of a photoelectrochemical solar cell. J. Appl. Phys. 59, 1570–1577.

Chen, Lin-Jer, Dai, Jia-Heng, 2017. Growth, morphological and optical characteristics of ZnSSe nanorods. Opt. Mater. 64, 356–360.

Da-ke, Shen, Sou, I.K., Gao-rong, Han, Pi-yi, Du, Duan-lin, Que, 2003. Polycrystalline ZnS_xSe_{1-x} thin films deposited on ITO glass by MBE. J. Zhejiang Uni.-Sci. A 4, 131–135.

Deshmukh, L.P., Shahane, G.S., 1997. $CdS_{1-x}Se_x$ thin film electrodes: an electrochemical photovoltaic study. Inter. J. Electronics 83, 341–350.

Deshmukh, L.P., Shahane, G.S., Garadkar, K.M., 1997. In-doped $CdS_{0.9}Se_{0.1}$photoelctrode for electrochemical solar cell applications. Ind. J. Pure App. Phy. 35, 560–564.

Dhanemozhi, Clara, John, Rita, Murali, K.R., 2017. Synthesis and characterization of ZnS_xSe_{1-x} films usinyg Brush plating technique. Mater. Today: Proc. 4, 5185–5189.

Fard, Zahra Asgari, Dehghani, Hossein, 2019. Investigation of the effect of Sr-doped in ZnSe layers to improve photovoltaic characteristics of ZnSe/CdS/CdSe/ZnSe quantum dot sensitized solar cells. Sol. Ener. 184, 378–390.

Franckevičius, Marius, Pakštas, Vidas, Grincienė, Giedrė, Kamarauskas, Egidijus, Giraitis, Raimondas, Nekrasovas, Jonas, Selskis, Algirdas, Juškėnas, Remigijus, Niaura, Gediminas, 2019. Efficiency improvement of superstrate CZTSSe solar cells processed by spray pyrolysis approach. Sol. Energy 185, 283–289.

Ganguly, A., Chaudhuri, S., Pal, A.K., 2001. Synthesis of ZnS_xSe_{1-x} (0 < x < 1) nanocrystalline thin films by high-pressure sputtering. J. Phys. D: Appl. Phys. 34, 506–513.

Ginley, D.S., Butler, M.A., 1981. Charge-transfer processes in photoelectrochemical cells. In: Nozik, A. (Ed.), Photoeffects at Semiconductor-Electrolyte Interfaces, ACS Symposium Series. American Chemical Society, Washington, DC.

Hankare, P.P., Chate, P.A., Chavan, P.A., Sathe, D.J., 2008. Chemical deposition of ZnSe thin films: Photoelectrochemical applications. J. Alloys Comp. 461, 623–627.

Hankare, P.P., Chate, P.A., Sathe, D.J., 2009. Effect of indium doping on photoelectrochemical properties of $Cd_{0.9}Zn_{0.1}Se$ photosensitive films. Phys. B 404, 2389–2394.

Hodes, Gary, 1980. A thin-film polycrystalline photoelectrochemical cell with 8% solar conversion efficiency. Nature 285, 29–30.

Iqbal, Muhammad Zahir, Rehman, Assad-Ur, 2018. Recent progress in graphene incorporated solar cell devices. Sol. Ener. 169, 634–647.

Isshiki, M., Wang, J., 2017. Wide-bandgap II-VI Semiconductors: Growth and Properties, Springer Handbook of Electronic and Photonic Materials. Springer, Cham.

Kamruzzaman, M., Dutta, R., Podder, J., 2012. Synthesis and characterization of the as-deposited $Cd_{1-x}Pb_xS$ thin films prepared by spray pyrolysis technique. Semiconductors 46, 957–961.

Karim, Nayab Abdul, Mehmood, Umer, Fizza Zahid, Hafiza, Asif, Tahira, 2019. Nanostructured photoanode and counter electrode materials for efficient dye-sensitized solar cells (DSSCs). Sol. Ener. 185, 165–188.

Kumar, Vipin, Sharma, T.P., 1998. Structural and optical properties of sintered ZnS_xSe_{1-x} films. Opt. Mater. 10, 253–256.

Liu, Qiang, Wang, Jinying, 2019. Dye-sensitized solar cells based on surficial TiO_2 modification. Sol. Ener. 184, 454–465.

Liu, Jun, Wei, Ai Xiang, Zhuang, Mi Xue, Zhao, Yu, 2013. Investigation of the ZnS_xSe_{1-x} thin films prepared by chemical bath deposition. J. Mater. Sci.: Mater. Electron. 24, 1348–1353.

Lohar, G.M., Dhaygude, H.D., Patil, R.A., Ma, Yuan-Ron, Fulari, V.J., 2015. Studies of properties of Fe^{2+} doped ZnSe nano-needles for photoelectrochemical cell application. J. Mater. Sci.: Mater. Electron. 26, 8904–8914.

Manivannan, R., Noyel Victoria, S., 2018. Preparation of chalcogenide thin films using electrodeposition method for solar cell applications – A review. Sol. Ener. 173, 1144–1157.

Mendil, R., Ben Ayadi, Z., Vázquez Vázquez, C., López Quintela, M.A., Djessas, K., 2018. A new procedure to synthesis of $ZnS_{1-x}Se_x$ nanoparticles by a facile solvothermal method. J. Mater. Sci.: Mater. Electron. 29, 10656–10662.

Murali, K.R., Thilagavathy, K., Vasantha, S., Gopalakrishnan, P., Rachel Oommen, P., 2010. Photoelectrochemical properties of CdS_xSe_{1-x} films. Sol. Energy 84, 722–729.

Pandey, R.N., Chandra Babu, K.S., Srivastava, O.N., 1996. High conversion efficiency photoelectrochemical solar cells. Prog. Surf. Sci. 52, 125–192.

Patil, N.M., Nilange, S.G., Yadav, A.A., 2018. Growth and characterization of ZnS_xSe_{1-x} thin films deposited by spray pyrolysis. Thin Solid Films 664, 19–26.

Patil, N.M., Nilange, S.G., Yadav, A.A., 2019. Properties of spray deposited ZnS_xSe_{1-x} thin films for photoelectrochemical solar cell application. J. Mater. Sci.: Mater. Electron. 30, 1647–1653.

Perednis, Dainius, Gauckler, Ludwig J., 2005. Thin film deposition using spray pyrolysis. J. Electroceramics 14, 103–111.

Ramakrishna Reddy, K.T., Subbaiah, Y.V., Reddy, T.B.S., Johnston, D., Forbes, I., Miles, R.W., 2003. Pyrolytic spray deposition of ZnS_xSe_{1-x} layers for photovoltaic applications. Thin Solid Films 431–432 pp. 340–343.

Sadekar, Harishchandra K., Ghule, Anil Vithal, Sharma, Ramphal, 2011. Bandgap engineering by substitution of S by Se in nanostructured $ZnS_{1-x}Se_x$ thin films grown by soft chemical route for nontoxic optoelectronic device applications. J. Alloys Comp. 509, 5525–5531.

Saikia, D., Raland, R.D., Borah, J.P., 2016. Influence of Fe doping on the structural, optical and magnetic properties of ZnS diluted magnetic semiconductor. Physica E 83, 56–63.

Siddiqui, Farha Y., Shaikh, Shaheed U., Upadhye, Deepak S., Huse, Nanasaheb P., Dive, Avinash S., Sharma, Ramphal, 2017. Investigation on the effect of copper doping on $CdS_{1-x}Se_x$thin films. Ferroelectrics 518, 153–162.

van de Krol, Roel, 2012. Principles of Photoelectrochemical Cells, Electronic Mater: Sci & Technology (Photoelectrochemical Hydrogen Production). Springer, pp. 13–67.

Venkata Subbaiah, Y.P., Prathap, P., Reddy, K.T.R., Mangalaraj, D., Kim, K., Yi, Junsin, 2007. Growth and characterization of ZnS_xSe_{1-x} films deposited by close-spaced evaporation. J. Phys. D Appl. Phys. 40, 3683–3688.

Venkata Subbaiah, Y.P., Prathap, P., Ramakrishna Reddy, K.T., Miles, R.W., Yi, J., 2008. Studies on $ZnS_{0.5}Se_{0.5}$ buffer based thin film solar cells. Thin Solid Films 516, 7060–7064.

Yadav, A.A., 2016. Photovoltaic characteristics of photoelectrochemical cell formed with indium-doped CdSSe thin film electrodes. J. Mater. Sci: Mater. Electron. 27, 4508–4515.

Yadav, A.A., Barote, M.A., Chavan, T.V., Masumdar, E.U., 2011. Influence of indium doping on the properties of spray deposited $CdS_{0.2}Se_{0.8}$ thin films. J. Alloys Comp. 509, 916–921.

Yadav, A.A., Masumdar, E.U., 2010. Photoelectrochemical performances of n-$CdS_{1-x}Se_x$ thin films prepared by spray pyrolysis technique. Sol. Ener. 84, 1445–1452.

Yadav, A.A., Masumdar, E.U., 2011. Photoelectrochemical performances of indium-doped $CdS_{0.2}Se_{0.8}$thin film electrodes prepared by spray pyrolysis. Electrochim. Acta 56, 6406–6410.